

Tunable Emission based on Lanthanide (III) Metal-Organic Frameworks: An Alternative Approach to White Lights

Song Dang,^a Jian-Han Zhang,^b and Zhong-Ming Sun,^{*a,b}

^aState Key Laboratory of Rare Earth Resource Utilization, Changchun Institute of Applied Chemistry, Chinese Academy of Sciences, 5625 Renmin Street, Changchun, Jilin 130022, P.R. China.

^bState Key Laboratory of Structural Chemistry, Fujian Institute of Research on the Structure of Matter, Chinese Academy of Sciences, Fuzhou 350002, P.R. China.

Table of Contents

1. Crystal data for Y(Er)L.....	S2
2. PXRD Analysis.....	S4
3. Luminescence Measurements.....	S4

1. Crystal data for Y(Er)L

Table S1. Bond lengths [Å] and angles [deg] for YL.

Y(1)-O(4)#1	2.314(5)	Y(1)-O(6)#5	2.436(3)
Y(1)-O(5)#2	2.340(3)	Y(1)-O(5)#4	2.449(3)
Y(1)-O(5)#3	2.340(3)	Y(1)-O(5)#5	2.449(3)
Y(1)-O(3)	2.373(5)	Y(1)-O(4)	2.414(5)
Y(1)-O(6)#4	2.436(3)	O(4)#1-Y(1)-O(5)#2	84.82(14)
O(4)#1-Y(1)-O(5)#3	84.82(14)	O(5)#2-Y(1)-O(5)#3	65.75(16)
O(4)#1-Y(1)-O(3)	152.24(17)	O(5)#2-Y(1)-O(3)	117.96(12)
O(5)#3-Y(1)-O(3)	117.96(12)	O(4)#1-Y(1)-O(4)	152.67(16)
O(5)#2-Y(1)-O(4)	72.36(13)		

Symmetry transformations used to generate equivalent atoms:

#1 $-x+1, -y+1, z+1/2$ #2 $x-1/2, y-1/2, z+1$ #3 $-x+3/2, y-1/2, z+1$
#4 $-x+3/2, -y+3/2, z+3/2$ #5 $x-1/2, -y+3/2, z+3/2$

Table S2. Bond lengths [Å] and angles [deg] for ErL.

Er(1)-O(1)	2.310(5)	Er(1)-O(3)	2.432(3)
Er(1)-O(2)#1	2.345(3)	Er(1)-O(2)#3	2.457(4)
Er(1)-O(2)#2	2.345(3)	Er(1)-O(2)	2.457(4)
Er(1)-O(6)#2	2.356(5)	Er(1)-C(11)#2	2.767(7)
Er(1)-O(1)#2	2.411(5)	Er(1)-C(12)#3	2.831(5)
Er(1)-O(3)#3	2.432(3)	Er(1)-C(12)	2.831(5)
O(1)-Er(1)-O(2)#1	84.41(14)	O(1)-Er(1)-O(2)#2	84.41(14)
O(2)#1-Er(1)-O(2)#2	66.04(16)	O(1)-Er(1)-O(6)#2	152.34(16)
O(2)#1-Er(1)-O(6)#2	118.22(12)	O(2)#2-Er(1)-O(6)#2	118.22(12)
O(1)-Er(1)-O(1)#2	152.24(16)	O(2)#1-Er(1)-O(1)#2	72.45(13)
O(2)#2-Er(1)-O(1)#2	72.45(13)	O(6)#2-Er(1)-O(1)#2	55.42(15)
O(1)-Er(1)-O(3)#3	101.65(14)	O(2)#1-Er(1)-O(3)#3	136.65(19)
O(2)#2-Er(1)-O(3)#3	71.85(17)	O(6)#2-Er(1)-O(3)#3	73.51(10)

Symmetry transformations used to generate equivalent atoms:

#1 $x, -y, z+1/2$ #2 $-x+2, -y, z+1/2$ #3 $-x+2, y, z$

Table S3. Cell parameters of all LnL.

$C_{108}H_{28}Ln_4O_{44}$ (Ln = Y, La, Pr, Nd, Eu, Gd, Tb, Dy, Ho, Er, Tm, Yb), Space group,
 $Cmc2_1$, $\alpha = \beta = \gamma = 90^\circ$

Ln	$a / \text{Å}$	$b / \text{Å}$	$c / \text{Å}$	$V / \text{Å}^3$
Y	18.036(6)	24.175(5)	6.986(6)	3046.464
La	17.97	23.82	7.521	3219.329
Pr	17.92	23.85	7.26	3102.866
Nd	18.07	24.16	7.273	3175.182
Eu	18.29	24.49	7.24	3242.956
Gd	17.90	23.85	7.06	3014.020
Tb	18.16	24.41	7.10	3147.328
Dy	18.03	24.23	7.02	3066.806
Ho	18.66	24.74	7.24	3342.334
Er	18.037(2)	24.308(3)	6.9817(9)	3061.154
Tm	18.03	22.90	7.02	2898.467
Yb	18.30	23.41	7.24	3083.184

2. PXRD Analysis

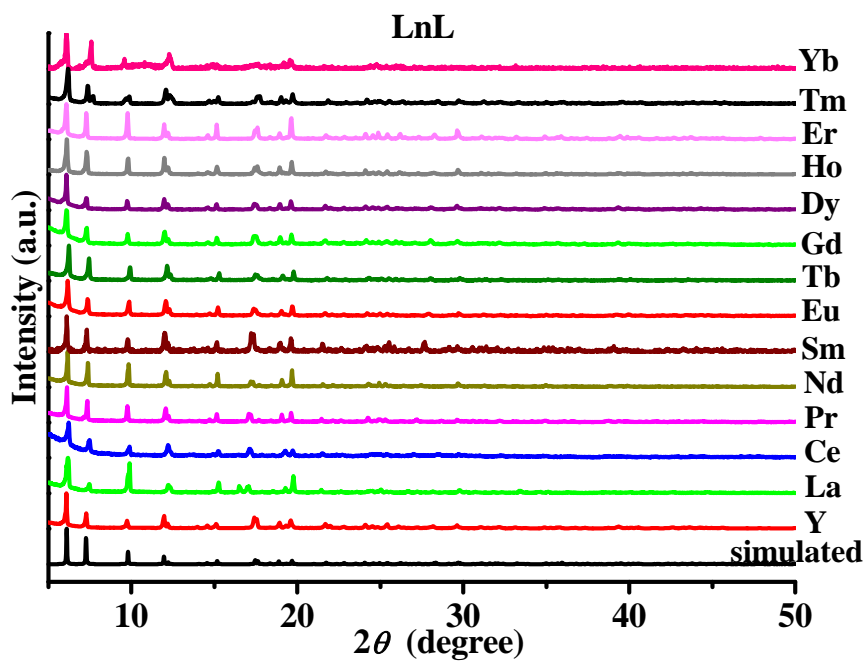


Fig. S1 Powder XRD patterns of compounds in the range from 5 to 50 degrees.

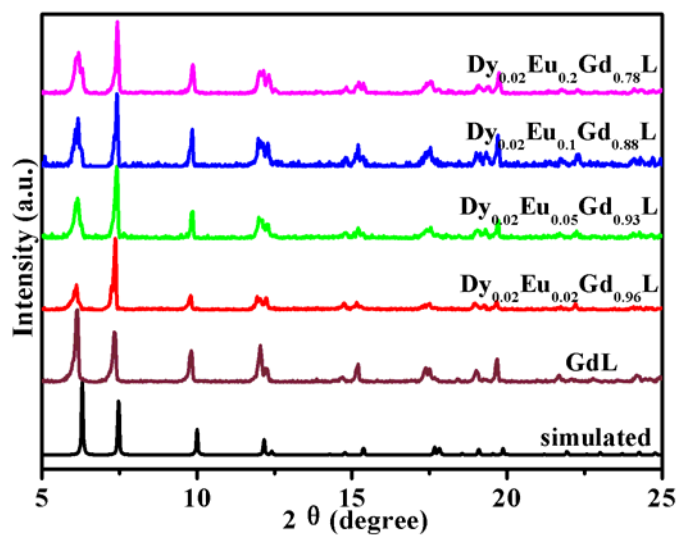


Fig. S2 Powder XRD patterns of Dy and Eu codoped compounds.

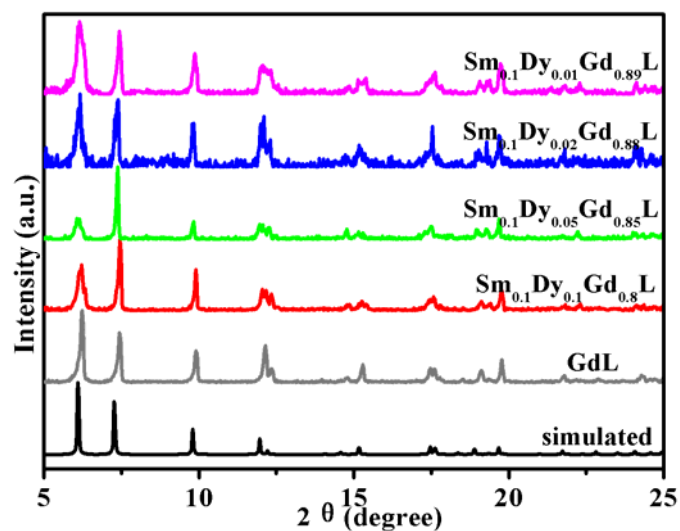


Fig. S3 Powder XRD patterns of Dy and Sm codoped compounds.

3. Luminescent Measurements

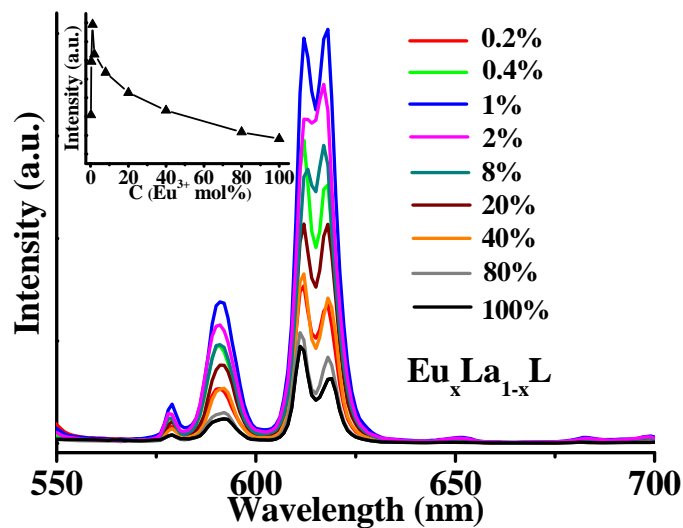


Fig. S4 PL emission spectra of $\text{Eu}_x\text{La}_{1-x}\text{L}$, solid samples. The inset figures indicate corresponding transition intensities of doped $\text{Eu}_x\text{La}_{1-x}\text{L}$ as a factor of doping concentration x .

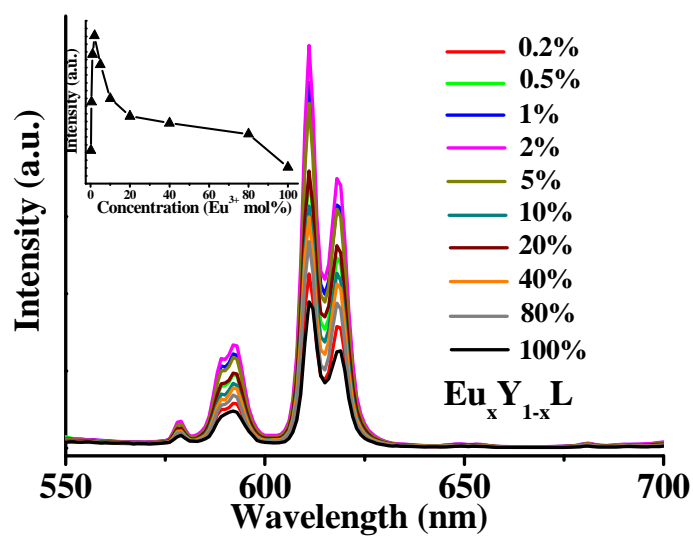


Fig. S5 PL emission spectra of $\text{Eu}_x\text{Y}_{1-x}\text{L}$, solid samples. The inset figures indicate corresponding transition intensities of doped $\text{Eu}_x\text{Y}_{1-x}\text{L}$ as a factor of doping concentration x .

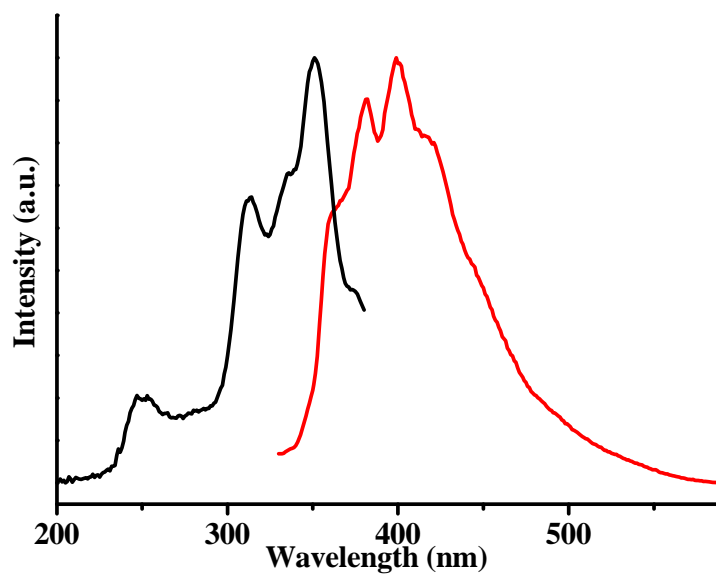


Fig. S6 Excitation (black, $\lambda_{\text{em}} = 400$ nm) and (red, $\lambda_{\text{ex}} = 310$ nm) emission spectra of H_3L .

Table S4. CIE coordinates of $\text{Dy}_x\text{Eu}_y\text{Gd}_{1-x-y}\text{L}$ ($\lambda_{\text{ex}} = 290 \text{ nm}$).

$\text{Dy}_x\text{Eu}_y\text{Gd}_{1-x-y}\text{L}$	CIE (X, Y)
$\text{Dy}_{0.02}\text{Eu}_{0.02}\text{Gd}_{0.96}\text{L}$	(0.310, 0.319)
$\text{Dy}_{0.02}\text{Eu}_{0.05}\text{Gd}_{0.93}\text{L}$	(0.355, 0.313)
$\text{Dy}_{0.02}\text{Eu}_{0.1}\text{Gd}_{0.88}\text{L}$	(0.373, 0.304)
$\text{Dy}_{0.02}\text{Eu}_{0.2}\text{Gd}_{0.78}\text{L}$	(0.379, 0.281)

Table S5. CIE coordinates of $\text{Sm}_x\text{Dy}_y\text{Gd}_{1-x-y}\text{L}$ ($\lambda_{\text{ex}} = 290 \text{ nm}$).

$\text{Sm}_x\text{Dy}_y\text{Gd}_{1-x-y}\text{L}$	CIE (X, Y)
$\text{Sm}_{0.1}\text{Dy}_{0.01}\text{Gd}_{0.89}\text{L}$	(0.350, 0.323)
$\text{Sm}_{0.1}\text{Dy}_{0.02}\text{Gd}_{0.88}\text{L}$	(0.319, 0.321)
$\text{Sm}_{0.1}\text{Dy}_{0.05}\text{Gd}_{0.85}\text{L}$	(0.306, 0.321)
$\text{Sm}_{0.1}\text{Dy}_{0.1}\text{Gd}_{0.8}\text{L}$	(0.292, 0.325)

Luminescence Decay measurements on the LnL and Ln^{3+} doped materials

The luminescence lifetimes have been recorded in order to explore the coordination environment around the lanthanide ions. The luminescence decay curves were fit well with monoexponential decays, using the following equation:

$$y = Ae^{(-x/t)} + y_0$$

which confirms that all lanthanide ions occupy the same average local environment with each samples.

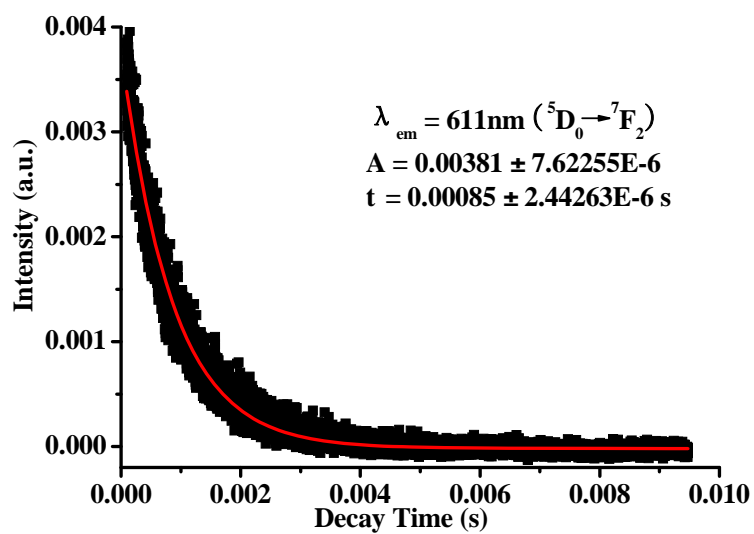


Fig. S7 Luminescence decay curve for the ${}^5D_0 \rightarrow {}^7F_2$ (611 nm) emission of EuL.

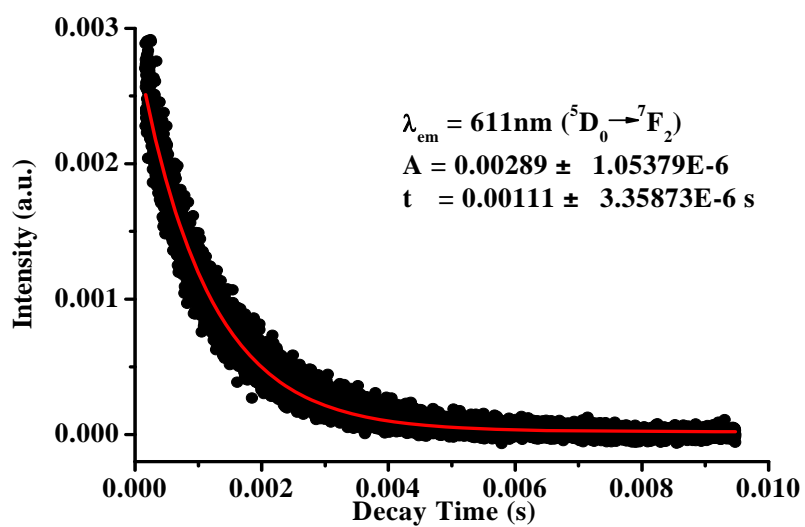


Fig. S8 Luminescence decay curve for the ${}^5D_0 \rightarrow {}^7F_2$ (611 nm) emission of Eu_{0.02}Gd_{0.98}L.

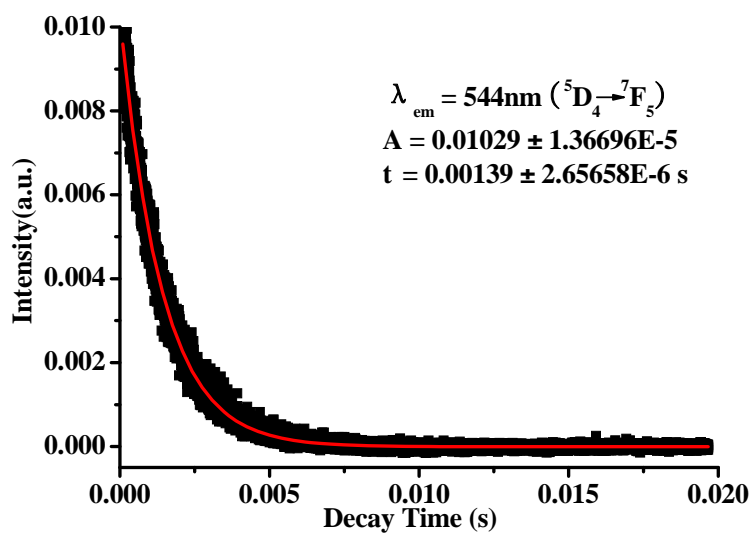


Fig. S9 Luminescence decay curve for the $^5D_4 \rightarrow ^7F_5$ (544 nm) emission of TbL.

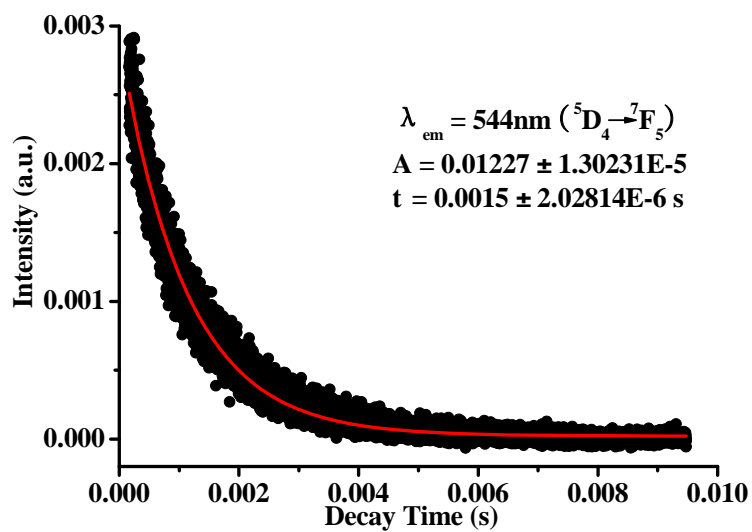


Fig. S10 Luminescence decay curve for the $^5D_4 \rightarrow ^7F_5$ (544 nm) emission of
Tb_{0.08}La_{0.92}L.

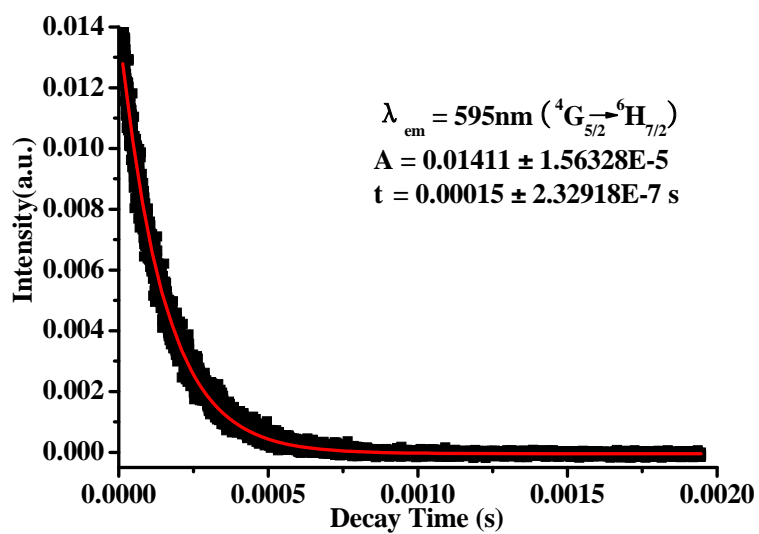


Fig. S11 Luminescence decay curve for the $^4G_{5/2} \rightarrow ^6H_{7/2}$ (595 nm) emission of $\text{Sm}_{0.1}\text{Gd}_{0.9}\text{L}$.

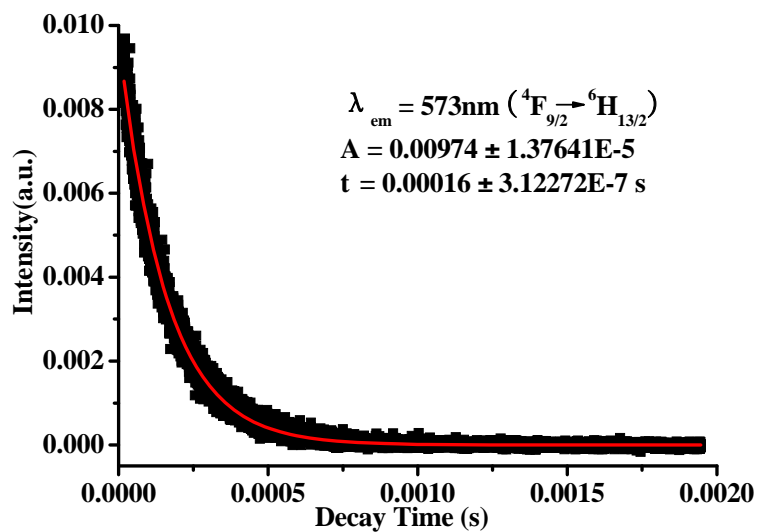


Fig. S12 Luminescence decay curve for the $^4F_{9/2} \rightarrow ^6H_{13/2}$ (573 nm) emission of $\text{Dy}_{0.02}\text{Gd}_{0.98}\text{L}$.